dielectric optical waveguides by the effective-index method," *Electron. Lett.*, vol. 15, no. 23, pp. 734–735, Nov. 8, 1979.
[10] E. A. J. Marcatili, "Bends in optical dielectric guides," *Bell Syst. Tech. J.*, vol. 48, pp. 2103–2132, Sept. 1969.
[11] R. M. Knox, P. P. Toulios, and J. Q. Howell, "Radiation losses in curved dielectric image waveguides of rectangular cross section," presented at the IEEE MTT-S Int. Microwave Symp., Boulder, CO, June 1973.
[12] H. Shinonaga and S. Kurazona, "*Y* dielectric waveguide for millimeter and submillimeter-wave," *IEEE Trans. Microwave Theory Tech.*, vol. MTT-29, pp. 542–546, June 1981.
[13] M. Tsuzi, S. Suhara, H. Shigesawa, and K. Takiyama, "Submillimeter guided-wave experiments with dielectric rib waveguides," *IEEE Trans. Microwave Theory Tech.*, vol. MTT-29, pp. 547–551, June 1981.
[14] K. Solbach and I. Wolff, "The electromagnetic fields and the phase constants of dielectric image lines," *IEEE Trans. Microwave Theory Tech.*, vol. MTT-26, pp. 266–274, Apr. 1978.
[15] "Special issue on open guided wave structures," *IEEE Trans. Microwave Theory Tech.*, vol. MTT-29, Sept. 1981.
[16] R. M. Knox, "Dielectric waveguide microwave integrated circuits—An overview," *IEEE Trans. Microwave Theory Tech.*, vol. MTT-24, pp. 806–814, Nov. 1976.
[17] R. A. Stern and R. W. Babbitt, "Dielectric waveguide circulator," *Int. J. Infrared and Millimeter Waves*, vol. 3, pp. 11–18, 1982.
[18] Y.-W. Chang and H. J. Kuno, "Millimeter-wave integrated circuits," U.S. Army Electronics Command, Final Rep. ECOM-74-0454-F, Oct. 1975.
[19] Y.-W. Chang, J. A. Pual, and Y. C. Ngan, "Millimeter-wave integrated circuit modules for communication interconnect systems," U.S. Army ERADCOM Final Rep. DELECT CR76-1353-F, 1978.
[20] Y.-W. Chang and L. T. Yuan, "Millimeter-wave integrated circuits," U.S. Army ERADCOM Final Rep. DELET-TR-78-3003-F, Oct. 1980.
[21] S. Dixon, Jr. and H. Jacobs, "Millimeter-wave InP image line self mixing Gunn oscillator," *IEEE Trans. Microwave Theory Tech.*, vol. MTT-29, pp. 958–961, Sept. 1981.
[22] P. P. Toulios and R. M. Knox, "Rectangular dielectric image lines for millimeter-wave integrated circuits," presented at the Western Electronics Show and Convention, Los Angeles, CA, Aug. 1970.

✤

Yu-Wen Chang (M'73) was born in China on December 1, 1938. He received the B.S. degree in engineering, the Ph.D. degree in solid-state electronics from the University of California, Los Angeles, in 1966 and 1971, respectively, and the M.S. degree in electrical engineering from the California Institute of Technology in 1967.

Presently, he is Engineering Staff Specialist at General Dynamics Pomona Division on Millimeter Wave Integrated Circuit Devices, Components, and Subsystems Development for Weapon System Applications. He was with TRW from 1978 to 1980 as Manager of Millimeter Wave Projects on Millimeter Wave Integrated Circuit Development. From 1973 to 1978 he was with Hughes Electron Dynamics Division as Senior Scientist in charge of Millimeter Wave Integrated Circuit Development.

Dr. Chang is a member of the American Physical Society.

Design of Dielectric Grating Antennas for Millimeter-Wave Applications

FELIX K. SCHWERING, MEMBER, IEEE, AND SONG-TSUEN PENG, SENIOR MEMBER, IEEE

Abstract—**A theoretical procedure well suited for generating design data on dielectric grating antennas for the millimeter-wave region is presented. The procedure utilizes the effective dielectric constant (EDC) method to determine the phase constant of the leaky modes supported by the antenna structure of finite lateral width. The radiation or leakage constant of these modes is obtained from the relatively simple boundary value problem of dielectric grating antennas of infinite width. For single-beam radiation, the practically interesting case, the phase and leakage constants completely determine the field distribution in the antenna aperture, from which the directivity gain and radiation pattern are then calculated. The dependence of the antenna characteristics on the dimensions of the radiating structure is presented and discussed for $\epsilon = 12$, the dielectric constant of typical millimeter-wave materials, such as silicon and GaAs.**

Manuscript received April 30, 1982; revised July 8, 1982. This work was supported in part by the Joint Services Electronics Program under Contract F49620-1 80-C-0077, and in part by the U.S. Army Laboratory Research Program under Contract DAAG 29-81-D-1 0100.

F. Schwering is with the U.S. Army Communications-Electronics Command, Fort Monmouth, NJ 07703.

S. T. Peng is with the Polytechnic Institute of New York, 333 Jay St., Brooklyn, NY 11201.

I. INTRODUCTION

RECENT ADVANCES in the fabrication of millimeter-wave systems using integrated-circuit technology have stimulated considerable interest in the development of new antenna configurations compatible with this technology [1]–[8]. If the antenna can be integrated with other components, the cost, size, and weight of the system can be greatly reduced. A dielectric waveguide with a periodic surface corrugation has been shown to hold substantial promise as a leaky-wave antenna for millimeter-wave applications [2]–[8]. Such an antenna structure may be conveniently fabricated on a uniform dielectric waveguide to form a completely integrated millimeter-wave system. In addition, these dielectric leaky-wave antennas offer the

0018-9480/83/0200-0199$01.00 ©1983 IEEE

advantage of electronic beam steering [2]–[3]. A considerable effort has been directed in recent years at better understanding this particular class of antennas and exploring its applications in millimeter-wave systems.

In this paper, we present a relatively simple design procedure for periodically corrugated image waveguides acting as a leaky-wave antenna. We recognize that this class of structures has been extensively analyzed for integrated optics applications as beam-to-surface-wave couplers, distributed feedback reflectors, and filters [9]. In fact, leaky-wave antennas and optical periodic couplers are based on the same physical principle, and a great deal of information on the basic wave characteristics of the optical devices can simply be carried over for the understanding of the millimeter-wave antennas. However, because of the substantial difference in the permittivity of the materials commonly used in the two frequency ranges and because of the different environments in which millimeter-wave antennas and optical periodic couplers are operated, these devices differ in many respects. The main purpose of this paper is to apply the results known for the optical counterpart [10]–[14] to the design of the millimeter-wave antennas, while appropriately taking into account the differences between the two frequency ranges.

Radiation from dielectric grating antennas is effected by the periodic perturbation of the waves guided by the uniform part of the waveguide structure, to be referred to as the unperturbed structure. This radiation occurs only in certain preferred directions, primarily determined by the phase constant of the unperturbed structure and the period of the perturbation. As a consequence of the associated radiation loss, the wave guided by the unperturbed structure must decay exponentially, as it propagates along the antenna. Therefore, the wave will exist with appreciable magnitude only over a finite length of the antenna, and a beam will be radiated with a beamwidth proportional to the decay constant of the guided wave. Conversely, the decay constant can be taken as a measure of the rate of energy leakage from the unperturbed structure and is often referred to as the leakage constant. Since the phase and decay constants determine the field distribution over the antenna aperture, they are the most important characteristics to be determined in the design of leaky-wave antennas.

Calculation of the exact radiation patterns of leaky-wave antennas of finite aperture is a difficult theoretical problem. The discontinuities at the entrance and exit ends, as well as the field extending beyond the side walls, will cause pattern distortions and increased sidelobe levels. On the other hand, under somewhat idealized conditions, pattern calculation becomes straightforward and the basic wave phenomena associated with this class of antennas can be considered well understood.

Consistent with the viewpoint and philosophy stated above, we analyze these antennas by a simple procedure that consists of three steps: the first is the use of the effective dielectric constant (EDC) method to determine the phase constant of the unperturbed uniform image waveguide for a preliminary design of the antenna configuration; the second is to determine the decay or leakage constant by the methods previously employed for optical periodic couplers; and finally, in the third step, the radiation patterns are determined from the field distribution in the antenna aperture [15]. We review first, in Section II, the theoretical background that includes various topics relevant to the overall goal of this work. In particular, the procedures for determining the propagation and radiation constants of periodic antennas will be discussed in some detail.

As stated earlier, a main thrust in ongoing millimeter-wave R&D is the full development of integrated-circuit technology. In order to facilitate integration of millimeter-wave antennas with other active and passive components, it is expected that these antennas will be fabricated from silicon or GaAs; these materials have a relatively high dielectric constant in the millimeter-wave region (roughly $\epsilon = 12$). Therefore, in Section III we concentrate on discussing parameter dependencies and obtaining design data for grating antennas of permittivity $\epsilon = 12$. Generalization to structures with lower dielectric constants is straightforward, and even better accuracy can be expected.

When the phase and decay constants have been determined the field distribution over the antenna aperture is in principle known. The far field radiation pattern of the antenna is then calculated in the usual manner by performing a spatial Fourier transform. Section IV presents results for cases of practical interest.

II. Theoretical Background

A periodically corrugated dielectric image waveguide is depicted in Fig. 1. For antenna applications, we assume the presence of a ground plane which will reflect any downward radiated energy into the upward direction. In this case, there is no need to design a special profile [16]–[19] of the teeth in order to eliminate downward radiation. Therefore, throughout this paper, we shall consider only rectangular teeth, i.e., a groove profile that can be made easily and precisely by machining. Regardless of how the antenna structure is fabricated, we shall take the view that it consists of two parts: one is the uniform image waveguide (unperturbed structure), and the other is the periodic layer. The uniform image waveguide has a rectangular cross section of height h and width w. The periodic layer has a thickness t, a period d, and a tooth width d_1. Finally, we shall consider explicitly only the special case where the periodic layer has the same width and the same dielectric constant as the uniform image waveguide, even though the theory described herein will be applicable also to periodic layers of different materials.

A. Characteristic Solution of Periodic Dielectric Waveguides

As an exact electromagnetic boundary value problem, periodic dielectric waveguides have been rigorously treated for the case of normal incidence (with respect to the direction of the grating grooves) and with the assumption that both the antenna structure and the source distribution do not depend on the coordinate parallel to the grooves (y-axis). Under these simplifying conditions, a general electromagnetic wave propagating in a periodic dielectric

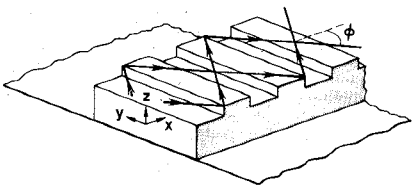

Fig. 1. Corrugated image guide of finite width. (For the antenna widths considered in this paper, $w \geq \lambda$, the angle ϕ will be relatively small.)

waveguide can be decomposed into independent TE and TM modes, which have been formulated in an exact fashion and analyzed extensively in the literature [9]–[14]. The advantage of the exact formulation is that it applies to gratings of arbitrary dimensions and constitutive parameters. A computer program based on the exact formulation is available; it was developed originally for the analysis of optical periodic couplers. Although this computer code requires relatively long computing times, it has been quite useful in establishing the accuracy of the various approximation techniques introduced subsequently. The computer program has been used for the same purpose in the present investigations of leaky-wave antennas for the millimeter-wave region.

While the assumption that both the structure and the source of excitation are uniform in the direction parallel to the grooves holds for most optical couplers, it is too restrictive for millimeter-wave grating antennas. The basic problem that has to be solved in the theory of gratings of finite width is the analysis of waves propagating at an oblique angle in a grating of infinite width [4]–[6]. This three-dimensional boundary value problem has only hybrid modes as solution, i.e., it involves coupling of TE and TM modes and cannot be reduced to the two-dimensional case. The problem has been formulated [4] and the effect of finite antenna width on the performance of grating antenna has been analyzed [6]. It has been shown in particular [5], [6] that the longitudinal phase constant is essentially that of the corresponding unperturbed structure and that the decay constant does not appreciably differ from that of a two-dimensional grating antenna (at normal incidence), as long as the antenna width is not very small. We shall assume in the following that this condition is satisfied, i.e., that w is in the order of a wavelength or larger.

B. Phase Constant of Grating Antennas

The uniform image waveguide belongs to the class of dielectric-strip waveguides for which a general method of analysis has been developed [20]–[23], and a new physical phenomenon of energy leakage has been shown to exist under appropriate conditions [22]–[24]. However, energy leakage will not take place in the image waveguide considered here. Therefore, the propagation constant is real in this case and can be determined with the help of approximate techniques, such as Marcatilli's method [25] or the EDC method [21]. We shall employ the EDC method throughout this paper since it yields the more accurate results for the antenna structures with which we are concerned; this applies to the whole frequency range of interest, including the cutoff region.

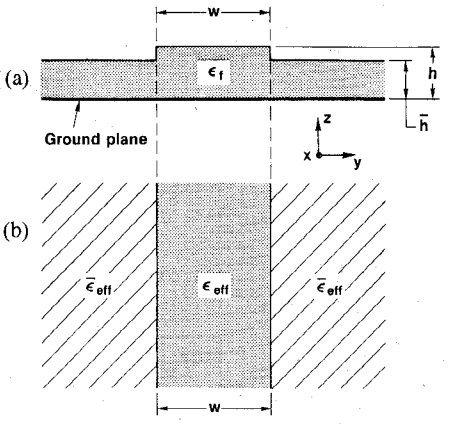

Fig. 2. Dielectric strip waveguide and the approximate EDC model. (a) Ridge guide and (b) EDC model.

The EDC technique is a simple method that employs transverse resonances to determine constituent transverse wavenumbers. To illustrate how this method is applied, let us consider the dielectric ridge waveguide of Fig. 2(a). One first views the cross section of the waveguide in terms of inside and outside regions, and then considers temporarily each of these uniform regions as being infinitely wide in the lateral direction. A transverse resonance in the *vertical* direction is then determined separately for the inside region of height h and for the outside region of height $\bar{h}$. As a result, the inside and outside regions are characterized in terms of effective dielectric constants ϵ_{eff} and $\bar{\epsilon}_{eff}$, respectively (indicating the axial propagation constants of the waves guided by the corresponding slab guides).

The next step in the EDC procedure is to neglect the presence of the step discontinuity at the sides of the waveguide, and to assume that the inside and outside regions, which are each now characterized as uniform homogeneous dielectric media with effective dielectric constants, are simply placed next to each other, as shown in Fig. 2(b). Now, we may effect a transverse resonance in the *horizontal* direction, and obtain the final value for the propagation constant k_x of the guided mode.

In the present case where we are considering antennas of the image guide type, the outside region has vanishing thickness $\bar{h} = 0$. Furthermore, to account for the effect of the periodic perturbation on the phase constant of the antenna, a layer of thickness t and uniform dielectric constant that is equal to the average dielectric constant ϵ_{ave} of the corrugated region is added on top of the original uniform layer forming the inside region. The modified uniform structure and its EDC model are shown in Fig. 3(a) and (b), respectively. The corresponding dispersion curves are presented in Fig. 4(a) and (b) and Fig. 5 and are discussed below. As mentioned before, we are restricting ourselves to silicon antennas with $\epsilon = 12$.

We first consider two limiting cases that are of conceptual interest. Fig. 4(a) shows the dispersion curves for the fundamental TM mode of a laterally unbounded dielectric layer of height h. Two different values are assumed for the dielectric constant of the region above the layer. The first value, $\epsilon_a = 1$, corresponds to the limiting case $t = 0$, where

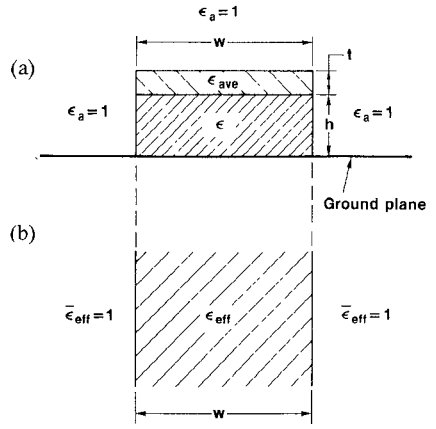

Fig. 3. Unperturbed image guide and its EDC model. (a) Unperturbed image guide and (b) EDC model.

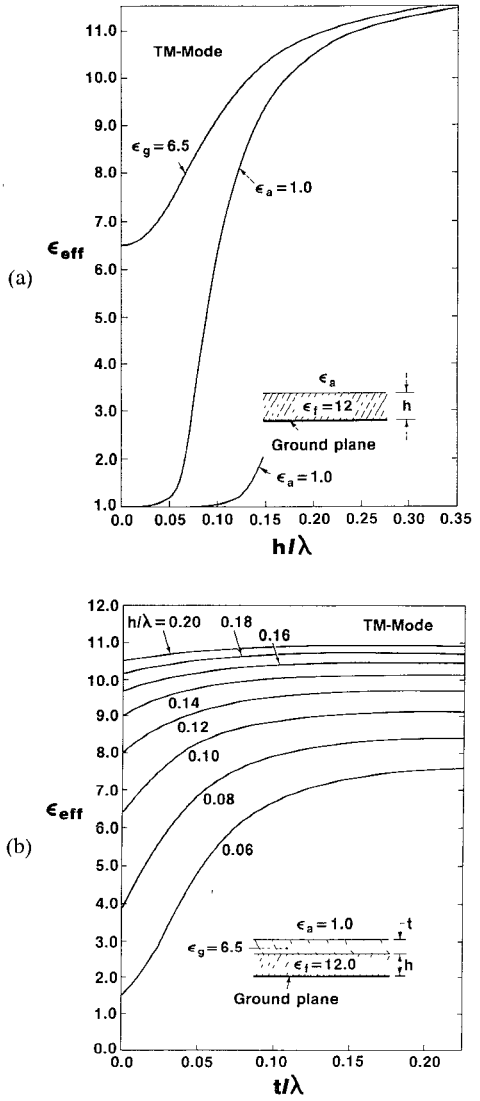

Fig. 4. TM-mode dispersion curves of two-dimensional layered structure. (a) Single layer with two different superstrates. (b) Double layer in air.

the perturbation layer of the antenna has vanishing thickness. The second value, $\epsilon_a = 6.5$, is the volume average dielectric constant of the corrugated region assuming an

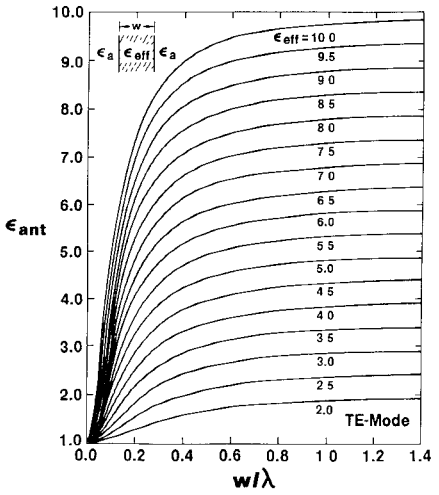

Fig. 5. TE-mode dispersion curves for various values of the dielectric constant.

aspect ratio $d_1/d = 0.5$; the corresponding dispersion curve applies to the limiting case $t \to \infty$. Evidently, for a finite corrugation-region thickness, $0 < t < \infty$, the dispersion curve must lie between these two curves which define the upper and lower bounds of the effective dielectric constant of the antenna. The dependence of ϵ_{eff} on t is shown in Fig. 4(b); the height h of the uniform portion of the antenna structure serves as a parameter in this graph.

For the second major step in the EDC method, i.e., the determination of the transverse resonance in the horizontal direction, the dispersion curves of the fundamental TE mode are needed for a slab waveguide of width w and permittivity ϵ_{eff}, where ϵ_{eff} has been determined in the first step (transverse resonance in the vertical direction). These dispersion curves are shown in Fig. 5 where ϵ_{ant}, the overall effective ϵ of the antenna, is plotted versus w for various values of ϵ_{eff}.

Figs. 4(b) and 5 provide all the information necessary for applying the EDC method to the (approximate) determination of the propagation constant of dielectric grating antennas. Comparison with the results of the (rigorous) computer method has confirmed the accuracy of the EDC technique.

C. Leakage Constant of Grating Antennas

While the propagation constant of dielectric grating antennas can be accurately determined from the EDC method, i.e., from an approximate technique which is easy to handle, calculation of the leakage constant requires a more rigorous solution of the problem. However, as pointed out in the first part of this section, the leakage constant of an antenna of finite width w can be approximated by that of an antenna of infinite width operated at normal rather than oblique incidence (with regard to the direction of the surface grooves). In this way, determination of the leakage constant can be reduced from a vector problem involving TE–TM coupling to a scalar problem in terms of TE waves or TM waves alone.

The theory of millimeter-wave grating antennas of infinite width can be adapted from the previously developed

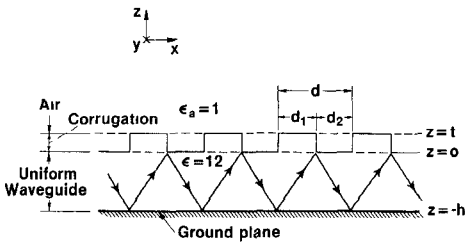

Fig. 6. Configuration of grating antennas.

analysis of optical periodic couplers [10]. The theory subdivides the total space range above the ground plane into three subregions (see Fig. 6): The uniform waveguide region $-h \le z \le 0$, the grating region $0 \le z \le t$, and the air half space $t \le z \le \infty$. Because of the periodicity of the antenna structure, the electromagnetic field in each of these regions can be written as a superposition of space harmonics. For TM modes we have

$$H_y(x,z) = \sum_{n=-\infty}^{+\infty} I_n^{(j)}(z) \exp(ik_{xn}x) \tag{1}$$

where $I_n^{(j)}$ is the magnetic field amplitude of the nth space harmonic in subregion j ($=1$, 2, or 3), and k_{xn} is the x-component of the complex wavenumber of this harmonic; k_{xn} is the same in the three subregions and is related to the wavenumber of the fundamental harmonic by

$$\begin{aligned} k_{xn} &= k_{x0} + 2\pi n/d \\ &= \beta - i\alpha + 2\pi n/d = \beta_n - i\alpha \end{aligned} \tag{2}$$

where β and α are the propagation and attenuation constants of the fundamental harmonic, respectively. Note that the propagation constant of the nth harmonic differs from that of any other harmonic but the attenuation constant α is the same for all harmonics.

By introducing the boundary condition that the tangential components of the electric and magnetic field strength must be continuous in the planes $z=0$ and $z=t$, and by formulating an appropriate radiation condition at $z \to \infty$, a homogeneous linear system is obtained for the space harmonics amplitudes $I_n^{(j)}$ in the three subregions. In other words, the problem is reduced to an eigenvalue problem; after appropriate truncation of the linear system, this problem can be solved numerically. The eigenvalues determine the complex wavenumber of the fundamental space harmonic, i.e., the propagation and leakage constant of the grating antenna, while the eigenvectors yield the amplitudes of the space harmonics in the three subregions $j=1$, 2, and 3.

Since the antennas considered here operate above a metal ground plane, they radiate into the upward direction only. As a consequence, it is unnecessary to explicitly determine the space harmonic amplitudes as long as we are interested in single-beam (i.e., single space harmonic) radiation only. Since this is the practically interesting case, we only have to determine the dispersion root $k_{x0} = \beta - i\alpha$ of the antenna; k_{x0} will be referred to as the complex wavenumber of the antenna. While the real part of k_{x0} can be obtained in good accuracy from the EDC method, the rigorous formulation is needed to determine the imaginary part, i.e., the leakage constant of the antenna. The computer program previously written for optical periodic couplers has been used to obtain this data for the millimeter-wave antennas considered here. Graphs showing the dependence of α on the antenna dimensions will be discussed in Section III.

D. Conditions for Single-Beam Radiation

In the grating region $0 \le z \le t$, the various space harmonics are mutually coupled by the boundary condition that E_{tang} and H_{tang} must be continuous at the vertical interfaces between teeth and grooves. In the air region, on the other hand, the medium is uniform and each harmonic propagates as an independent plane wave. The transverse propagation constant of the nth harmonic is given by

$$k_{zn} = \left(k_0^2 - k_{xn}^2\right)^{1/2}. \tag{3}$$

For a shallow corrugation, i.e., when t is small, it is intuitively clear that $\alpha \approx 0$ and $k_{x0} \approx \beta$, where β is the longitudinal propagation constant of the unperturbed structure, as shown in Fig. 3(a). In this case we obtain, from (2) and (3)

$$k_{zn} = k_0 \left[1 - \left(n_{\text{ant}} + n\frac{\lambda}{d}\right)^2\right]^{1/2} \tag{4}$$

where $n_{\text{ant}} = \sqrt{\epsilon_{\text{ant}}} = \beta/k_0$ is the effective refractive index of the unperturbed structure. Single-beam operation implies that only the $n=-1$ harmonic radiates. Hence, we must have $k_{z,-1}$ real, while all k_{zn} with $n \neq -1$ are imaginary. This requirement imposes the following condition on the corrugation period d:

$$\frac{\lambda}{n_{\text{ant}}+1} \le d \le \frac{\lambda}{n_{\text{ant}}-1}, \qquad \text{for } n_{\text{ant}} > 3 \tag{5}$$

$$\frac{\lambda}{n_{\text{ant}}+1} \le d \le \frac{2\lambda}{n_{\text{ant}}+1}, \qquad \text{for } n_{\text{ant}} < 3. \tag{6}$$

Although these formulas are derived under the assumption that t is very small, they also hold in good approximation for large t, except when α becomes large. For most practical cases, where t is smaller than h and small compared to λ, (5) and (6) should give a fairly accurate estimate of the range of admissible d values.

For the set of values for n_{ant} and d satisfying either (5) or (6), the $n=-1$ harmonic radiates into the air region at an angle (with respect to the z-axis)

$$\phi_{-1} = \sin^{-1}(\beta_{-1}/k_0) = \sin^{-1}(n_{\text{ant}} - \lambda/d). \tag{7}$$

The sign of ϕ_{-1} determines whether forward or backward radiation is obtained.

III. Design of Leaky-Wave Antennas

Since we are restricting ourselves to antennas of given permittivity ($\epsilon=12$), the antenna configuration is characterized by four geometrical parameters: the height of the uniform waveguide h; the thickness of the corrugation region t; the period of the corrugation d; and the aspect

ratio d_1/d. We shall determine the effect of each of these parameters on the antenna characteristics. The free-space wavelength is regarded here as a normalization parameter of the antenna dimensions.

The influence of the antenna width w on the complex wavenumber $k_{x0} = \beta - i\alpha$, and on the field distribution within the antenna in general, is small since we have assumed that w is in the order of λ. See for example Fig. 5, which shows that for $w > \lambda$: $\epsilon_{ant} \approx \epsilon_{eff}$, so that the effective dielectric constant is practically independent of the antenna width.

A. Effect of Waveguide Height h

From Fig. 4(a), we observe that $h \leq 0.2\lambda$ will ensure the existence of only the fundamental mode, if the corrugation thickness is not very large. We further observe that a larger value of h/λ will yield a smaller change in ϵ_{eff} in response to a change in h/λ. This means physically that at high frequencies, the waveguide height does not appreciably affect the fundamental guided mode and that fabrication tolerances will not be a serious problem. On the other hand, if frequency scanning of the antenna beam is a main objective, (7) shows that λ should be chosen such that ϵ_{eff} changes most rapidly with λ. This means that h/λ should be small ($h/\lambda \approx 0.1$). Choosing h/λ will therefore involve a tradeoff between fabrication tolerances and scan range.

Moreover, the choice of h/λ will have a strong influence on the field distribution of a guided wave. Near cutoff, i.e., at low frequencies, most of the field energy is transmitted in the air region, while at high frequencies the field is mostly concentrated within the uniform dielectric. In these two extreme cases, the field in the corrugation region is expected to be very weak and so is the radiation. In other words, we can expect that for a given waveguide height h, the radiation will peak at an intermediate frequency or, conversely, at a given frequency there exists an optimum waveguide height h providing the strongest radiation. Fig. 7 shows the variation of the phase constant (radiation angle) and leakage constant with changing waveguide height h. For the set of parameters indicated, the radiation peaks at $h/\lambda = 0.208$. The corresponding radiation angle is 46°. Furthermore, we observe that a change of 10 percent in h/λ will reduce the radiation rate to less than half its peak value, while the change in radiation angle is relatively small. Evidently, in this case, the thickness of the uniform layer is an important parameter for the control of the radiation rate while it does not significantly affect the radiation angle.

B. Effect of Grating Thickness

Fig. 7 shows that a reasonable thickness of the uniform layer is $h/\lambda = 0.2$; we shall assume this value in the following discussion. It is known from the literature [9]–[14] that the radiation rate α is proportional to t^2, for small t, and that it reaches a saturation value for large t, provided the guided-wave field remains evanescent in the corrugation region. For the aspect ratio $d_1/d = 0.5$, the average dielectric constant of the grating region is $\epsilon_{ave} = 6.5$,

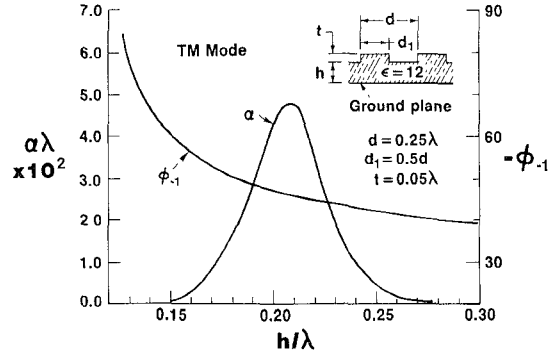

Fig. 7. Variations of phase and attenuation constants with waveguide height.

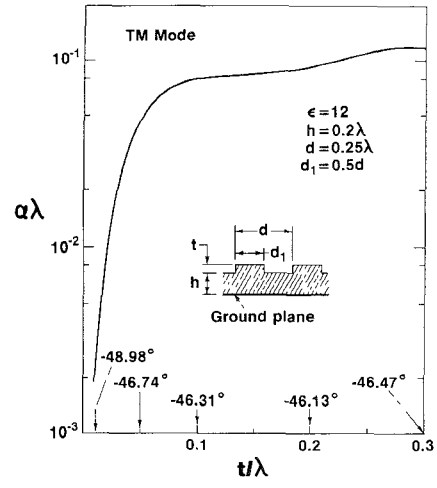

Fig. 8. Variations of phase and attenuation constants with grating thickness.

and the guided-wave field is indeed evanescent in this region. Fig. 8 shows the radiation constant α as a function of t. It is evident that the radiation rate varies with corrugation thickness in the expected fashion.

C. Effect of Grating Period d

With the principle of grating antennas based on the periodic nature of these structures, it can be expected that the period of the corrugation is the most important design parameter of this class of antennas.

According to (5) and (6), the choice of d determines whether single- or multiple-beam radiation is obtained; and, according to (7), d has a determining influence on the radiation angle ϕ_{-1} and, thus, on the propagation constant β. The dependence of the leakage constant α on d is plotted in Fig. 9(a) and (b) assuming $h = 0.2\lambda$, $t = 0.05\lambda$, which insures the existence of only the fundamental mode. For completeness, some radiation angles ϕ_{-1} are indicated in these figures.

Fig. 9(a) shows that $\alpha\lambda$ is in the order of 0.1 over a large range of d/λ values. This has consequences concerning antenna size and efficiency. For a grating antenna to be efficient, its axial length must be sufficiently large, i.e., most of the guided power must be radiated out before it reaches the antenna termination at the far end (where the remaining power is absorbed in order to avoid pattern

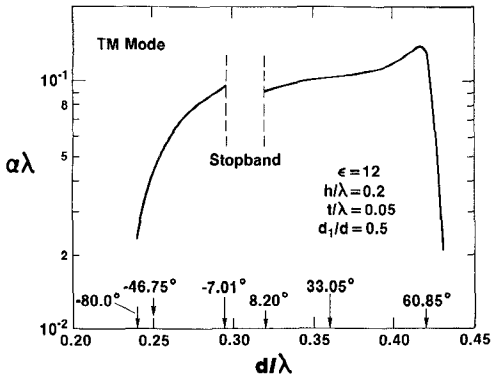

(a)

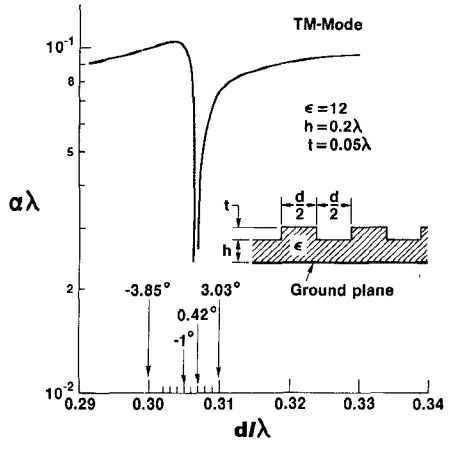

(b)

Fig. 9. Variations of phase and attenuation constant with grating period. (a) Dependence of leakage constant α on d. (b) Leakage constant in immediate vicinity of stopband.

distortions). The axial length required to obtain a given efficiency η is

$$L = -\frac{1}{2\alpha}\ln(1-\eta)$$

where dielectric losses have been neglected. If $\alpha\lambda = 0.1$, then $L/\lambda = 11.5$ for $\eta = 90$ percent, and $L/\lambda = 23$ for $\eta = 99$ percent. This leads to very reasonable antenna dimensions even in the lower millimeter-wave region near $\lambda = 1$ cm.[1] The large $\alpha\lambda$ values of Fig. 9(a) are a consequence of the high dielectric constant considered here ($\epsilon = 12$). Computations for a boron nitride antenna with $\epsilon = 4$ have yielded $\alpha\lambda$-values by an order of magnitude smaller, i.e., in the order of 0.01. High efficiency would require rather large antennas in this case.

Fig. 9(a) also confirms the well-known fact that periodic antennas do not radiate in the boreside direction $\phi_{-1} = 0$. As boreside conditions are approached an internal resonance develops leading to a stopband, i.e., the reflection coefficient of the antenna approaches unity. Fig. 9(b) shows the leakage constant in the immediate vicinity of the stopband. Apparently the stopband is very narrow. For $|\phi_{-1}| \geq 2.5°$ near normal values of $\alpha\lambda$ are restored.

[1]The effects of $\alpha\lambda$ and L/λ on the directivity and beamwidth of the antenna are discussed in Section IV.

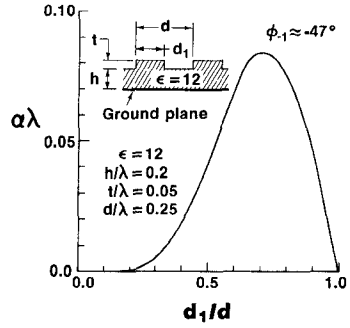

Fig. 10. Variations of phase and attenuation constants with aspect ratio.

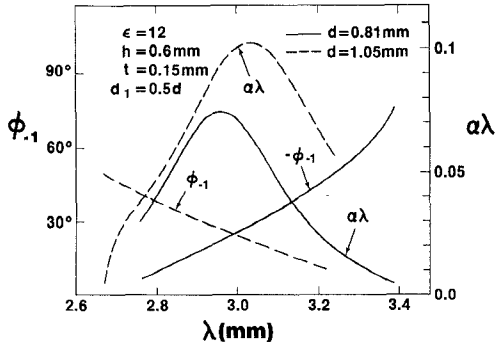

Fig. 11. Variations of phase and attenuation constants with wavelength.

D. Effect of Aspect Ratio

In the two limiting cases of the aspect ratio, $d_1/d = 0$ and 1, the periodic structure becomes uniform and no radiation can occur. For optical structures with a relatively low dielectric constant, it is well known that maximum radiation occurs at $d_1/d = 0.5$ [14]. For millimeter-wave antennas, however, the dielectric constant is relatively high and the field varies strongly across the grating region which leads to a significant change in the functional dependence of the leakage constant on aspect ratio (see Fig. 10). For $\epsilon = 12$, the field is evanescent in the grating region for $d_1/d = 0.5$, and the radiation rate is greatly reduced. The maximum of $\alpha\lambda$ has shifted to $d_1/d = 0.7$. Hence, to obtain a large radiation rate, the grooves should be chosen relatively narrow.

E. Frequency Scanning

A particular advantage of grating antennas is that their radiation pattern can be scanned electronically by changing frequency. We discuss this scan capability by using a specific example, i.e., a silicon antenna with grating period $d = 0.81$ mm for backward radiation and $d = 1.05$ mm for forward radiation. The antenna is assumed to be operated in the 3-mm region (94-GHz band) and to be designed for single-beam operation. Fig. 11 shows the radiation angle ϕ_{-1} as a function of λ for both grating periods. In addition, the leakage constant α is plotted versus λ. The leakage constant is of importance since, for efficient antennas of sufficient axial length, it determines the beamwidth of the main beam and its variation with scan angle.

The figure shows that for a 10-percent change in wave-

length, say from $\lambda = 2.85$ mm to 3.15 mm, the main beam direction sweeps almost linearily over an angular range of about 25° for backward radiation and 20° for forward radiation. In both cases, the leakage constant reaches a peak value near $\lambda = 3$ mm and decreases almost symmetrically from this maximum as the wavelength changes. This is a very desirable characteristic. If we designate the $\lambda = 3$-mm wavelength as the center wavelength of a frequency scan, the α values and, thus, the beamwidth will change comparatively little as the antenna is scanned and a stable radiation pattern with little beam distortions can be expected.

IV. Radiation Pattern

A grating antenna of finite length L and width w is shown in Fig. 12(a). It is assumed here that the antenna is fed by and terminates into uniform dielectric waveguides of the same height, width, and permittivity as the antenna itself. Furthermore, we assume that only one leaky-wave mode is excited in the antenna. This mode can be expressed as a superposition of space harmonics according to (1). In the "antenna aperture", i.e., in the portion of the plane $z = t$ located just above the antenna, the magnetic field strength takes the form

$$H_y(x, y, t) = e^{-\alpha x} \sum_{n=-\infty}^{+\infty} I_n e^{-i\beta_n x} \cos\left(\frac{\pi y}{w}\right) \tag{8}$$

for

$$0 \le x \le L, \quad -\frac{w}{2} \le y \le +\frac{w}{2}, \quad z = t$$

with

$$\beta_n = \beta + \frac{2\pi n}{d}.$$

The complex wavenumber $\beta - i\alpha$ and the space harmonics amplitudes I_n are determined by the eigenvalue problem described in the Section II-C. The y-dependence of H_y is approximate but should be accurate if w is sufficiently large ($w > \lambda$). Furthermore, any effects of the antenna-to-waveguide transitions at $x = 0$ and L on the aperture field of the antenna have been disregarded.

As stated before, the antenna dimensions are chosen such that only the $n = -1$ space harmonic will radiate. Hence, for the calculation of the radiation pattern, the field distribution in the plane $z = t$ can be approximated by the contribution of the $n = -1$ space harmonic alone

$$H_y(x, y, t) = \begin{cases} I_{-1} e^{-\alpha x} e^{-ik_0 x \sin\phi_{-1}} \cos\left(\dfrac{\pi y}{w}\right), \\ \qquad \text{for } 0 \le x \le L, \quad |y| \le \dfrac{w}{2} \\ 0, \qquad \text{elsewhere.} \end{cases} \tag{9}$$

Here we have used (7) to replace $\beta - 2\pi/d$ by $k_0 \sin\phi_{-1}$.

The approximations involved in (9) require further discussion. In actuality, the surface wave guided by the feeding and terminating waveguides and the space harmonics of order $n \neq -1$ of the antenna will contribute to the magnetic field distribution in the plane $z = t$. Since antenna and waveguides are of finite or semi-infinite (rather than infinite) length, these fields, though exponentially decaying in the z-direction, will in principle contribute to the radiation pattern and so will the fields scattered at the antenna-to-waveguide transitions. These contributions are neglected here because the antenna length L is large compared to λ and since any transitions can be made gradual by tapering the depth of the corrugations. Only spurious radiation will result which will have little effect on the mainbeam (though it can have a strong effect on pattern shape in the sidelobe region and, in particular, in the far sidelobe region where power levels are substantially reduced).

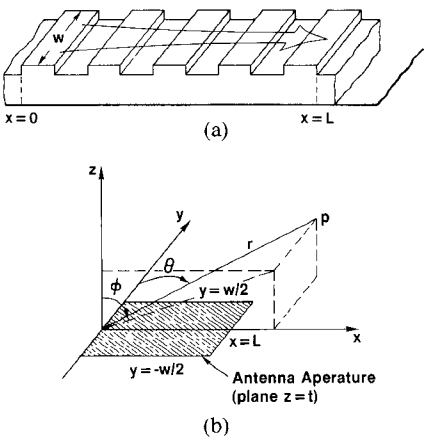

Fig. 12. Antenna aperture and coordinate system for far field calculation. (a) Grating antenna of finite length L and width w. (b) Antenna aperture.

Calculation of the radiation pattern from field distribution (9) is straightforward; details are given in Appendix. The power radiation pattern of the antenna is obtained in the form

$$G(\theta, \phi) = G_D S(\cos\theta) T(\sin\phi \sin\theta)$$

where

$$G_D = \frac{16}{\pi^3} k_0^2 \frac{w}{\alpha} \tanh\left(\frac{\alpha L}{2}\right) \cos\phi_{-1}$$

is the directivity gain of the antenna and

$$T(\sin\phi\sin\theta) = \left(\frac{\alpha L}{1 - e^{-\alpha L}}\right)^2 \cdot \frac{1 - 2e^{-\alpha L}\cos\left[k_0 L(\sin\phi\sin\theta - \sin\phi_{-1})\right] + e^{-2\alpha L}}{(\alpha L)^2 + (k_0 L)^2(\sin\phi\sin\theta - \sin\phi_{-1})^2}$$

is the E-plane pattern and

$$S(\cos\theta) = \left(\frac{\pi}{2}\right)^4 \frac{\cos^2\left(\dfrac{k_0 w}{2}\cos\theta\right)}{\left\{\left(\dfrac{\pi}{2}\right)^2 - \left(\dfrac{k_0 w}{2}\cos\theta\right)^2\right\}^2} \sin^2\theta$$

is the H-plane pattern; θ and ϕ are spherical coordinates as indicated in Fig. 12(b). Both S and T are normalized to unity in the main beam direction $\theta = 90°$, $\phi = \phi_{-1}$.

The H-plane pattern is the well-known radiation char-

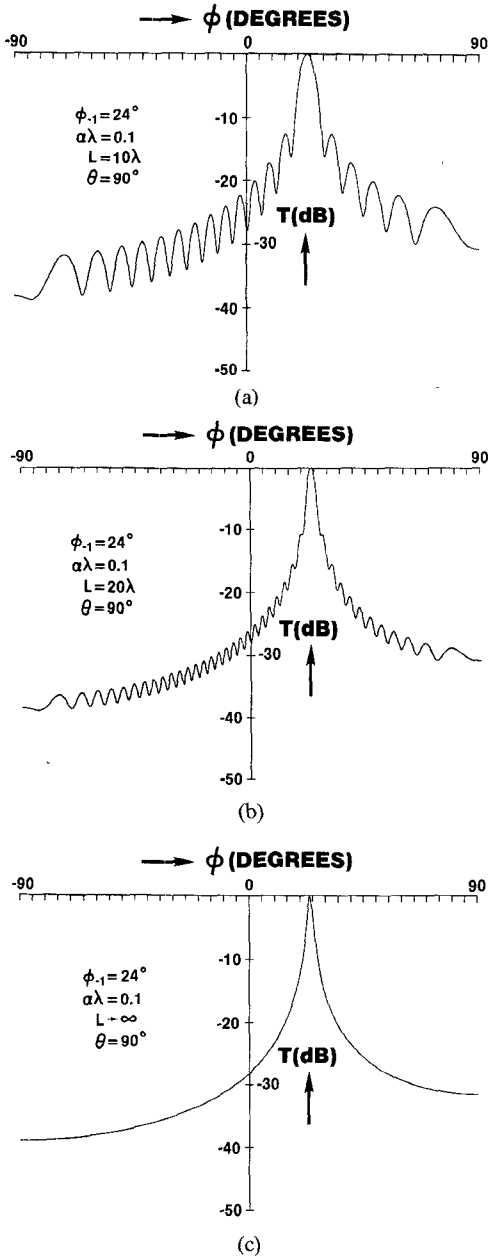

Fig. 13. E-plane pattern for $\phi_{-1} = 24°$, $\alpha\lambda = 0.1$ and (a) $L = 10\lambda$, (b) $L = 20\lambda$, (c) $L = 150\lambda$.

acteristic of a cos-tapered source distribution. Its 3-dB beamwidth is $\Delta\theta = 2\pi/(k_0 w)$ and all sidelobes are below -23 dB. The E-plane pattern is that of an exponentially tapered source distribution. This pattern is plotted in Fig. 13(a)–(c) for various values of L assuming a leakage constant $\alpha\lambda = 0.1$. For the L-values considered in these figures ($L \geq 10\lambda$), the antenna efficiency $\eta = 1 - e^{-2\alpha L}$ exceeds 85 percent, and the 3-dB beamwidth is in the order of a few degrees, which is appropriate for most millimeter-wave applications. A narrower beamwidth is, in principle, easily realizable by reducing the leakage constant α and correspondingly increasing $L(\sim 1/\alpha)$. The opposite case, where a broader beamwidth is required, poses more of a problem: either α would have to be increased beyond $\alpha\lambda = 0.1$, which is already close to the maximum value for antennas with $\epsilon = 12$, or the antenna length L would have to be reduced at the expense of a decreased efficiency η. First sidelobes of the E-plane pattern are down by only -13 dB.[1] However, these sidelobes degenerate into small shoulders as the antenna length is increased and the field strength at the far end of the antenna becomes smaller and smaller. If $\alpha L \gg 1$, so that practically all of the input power is radiated and less than 1 percent remains to be absorbed in the antenna termination, the sidelobes completely disappear and, within the approximation used, a very smooth pattern is obtained (see Fig. 13(c)). Of course, pattern shaping is possible by tapering the depth of the surface corrugation or its aspect ratio d_1/d while maintaining d as a constant (to preserve periodicity). This possibility, however, is not studied in this paper.

As should be expected, the directivity gain G_D is proportional to the antenna aperture area $2wL$, as long as $\alpha L \ll 1$, and the aperture illumination is practically uniform (low efficiency case). In the opposite case that $\alpha L \gg 1$, the effective length of the antenna is determined by the decay constant α. Accordingly, G_D is proportional to $2w/\alpha$ in this case, and independent of L.

Appendix
Radiation Pattern Calculation

With the tangential magnetic (or electric) field distribution in the aperture plane of the antenna $z = t$ known, the field distribution in the air halfspace $z > t$ can be formulated as a surface integral involving the well-known Green's function of a plane screen as a kernel. The far-zone field is obtained by evaluating this integral asymptotically for $kr \to \infty$. Using the spherical coordinate system in Fig. 12(b), and assuming that the magnetic field distribution in the antenna aperture has a y-component only, we obtain

$$E_\phi = -\sqrt{\frac{\mu}{\epsilon}}\, H_\theta = \frac{ik_0}{2\pi}\sqrt{\frac{\mu}{\epsilon}}\,\frac{e^{-ik_0 r}}{r} R(\theta,\phi) \qquad \text{(A1)}$$

with

$$R(\theta,\phi) = \sin\theta \int\int_{-\infty}^{+\infty} H_y(x^1, y^1, t) \cdot e^{ik_0[x^1 \sin\phi \sin\theta + y^1 \cos\theta]}\, dx^1\, dy^1 \qquad \text{for } k_0 r \to \infty. \qquad \text{(A2)}$$

The remaining field components are negligible. $R(\theta,\phi)$ is the field strength radiation pattern which is related to the aperture distribution of the antenna by a Fourier transform. We represent the power radiation pattern by the directivity gain function

$$G(\theta,\phi) = \frac{4\pi r^2 S_p(r,\theta,\phi)}{P_A} \qquad \text{(A3)}$$

[2]This comparatively high sidelobe level is due to the assumption inherent in (9) that the aperture distribution of the antenna abruptly ends with a discontinuity at $x = L$. A more gradual behavior of the aperture distribution at the antenna-to-waveguide transitions could be simulated by multiplying the right side of (9) with a weighting function of the form $\sin(\pi x/L)$. The aperture distribution would then be continuous at $x = 0$ and L, and the first sidelobes of the E-plane pattern would be reduced to -23 dB.

where

$$S_{P_y} = -E_\phi H_\theta^* = \sqrt{\frac{\epsilon}{\mu}}\, E_\phi E_\phi^*$$

is the Poynting vector, and

$$P_A = r^2 \int_{\theta=0}^{\pi} \int_{\phi=-\pi/2}^{+\pi/2} S_P(r,\theta,\phi) \sin\theta \, d\theta \, d\phi \qquad \text{(A4)}$$

is the total radiated power of the antenna. Using (9) for the aperture distribution of H_y, the integrals on the right side of (A2) can be evaluated in closed form, and the power radiation pattern (A3) can be formulated. Calculation of the total power P_4 requires an additional integration which can be performed approximately by considering that the major portion of the antenna power is radiated in the vicinity of the mainbeam direction $\theta = \pi/2$, $\phi = \phi_{-1}$. We thus obtain

$$S(r,\theta,\phi) = \frac{k_0^2}{\pi^4 r^2} \sqrt{\frac{\mu}{\epsilon}}\, |I_{-1}|^2 \left(\frac{w}{\alpha}\right)^2 (1 - e^{-\alpha L})^2 \cdot S(\cos\theta) T(\sin\phi \sin\theta)$$

$$P_A = \frac{1}{4} \sqrt{\frac{\mu}{\epsilon}}\, |I_{-1}|^2 \frac{w}{\alpha \cos\phi_{-1}} (1 - e^{-2\alpha L})$$

where

$$S(\cos\theta) = \left(\frac{\pi}{2}\right)^4 \frac{\cos^2\left[\frac{k_0 w}{2}\cos\theta\right]}{\left\{\left(\frac{\pi}{2}\right)^2 - \left(\frac{k_0 w}{2}\cos\theta\right)^2\right\}^2} \sin^2\theta$$

$$T(\sin\phi\sin\theta) = \left(\frac{\alpha L}{1 - e^{-\alpha L}}\right)^2 \cdot \frac{1 - e^{-\alpha L}\cos\left[k_0 L(\sin\phi\sin\theta - \sin\phi_{-1})\right] + e^{-2\alpha L}}{(\alpha L)^2 + (k_0 L)^2 (\sin\phi\sin\theta - \sin\phi_{-1})^2}.$$

S and T have been normalized to be unity in the main beam direction. Hence, the power radiation characteristic ((A3)) takes the form

$$G(\theta,\phi) = G_D S(\cos\theta) T(\sin\phi\sin\theta) \qquad \text{(A5)}$$

where

$$G_D = \frac{16}{\pi^3} k_0^2 \frac{w}{\alpha} \tanh\left(\frac{\alpha L}{2}\right) \cos\phi_{-1}$$

is the directivity gain of the antenna. The function $S(\cos\theta)$ determines the H-plane pattern and the function $T(\sin\phi \cdot \sin\theta)$ the E-plane pattern of the antenna. Graphs of the E-plane pattern are shown in Figs. 13(a)–(c). The H-plane pattern is the well-known radiation characteristic of a cos-tapered aperture illumination.

REFERENCES

[1] H. Jacobs and M. M. Chrepta, "Semiconductor dielectric waveguides for millimeter-wave functional circuits," in *IEEE Int. Microwave Symp. Dig*, 1973, p 28

[2] K. L. Klohn, R. E. Horn, H. Jacobs, and E. Freibergs, "Silicon waveguide frequency scanning linear array antenna," *IEEE Trans. Microwave Theory Tech.*, vol MTT-26, pp. 764–773, 1978.

[3] R. E. Horn, H. Jacobs, E. Freibergs, and K. L. Klohn, "Electronic modulated beam-steerable silicon-waveguide array antenna," *IEEE Trans. Microwave Theory Tech.*, vol. MTT-28, pp. 647–653, 1980.

[4a] S. T. Peng and F. Schwering, "Dielectric grating antennas," U.S. Army CORADCOM, Ft. Monmouth, NJ, R&D Tech Rep CORADCOM 78-3, 1978.

[4b] S. T. Peng, "Oblique guidance of surface waves on corrugated dielectric layers," in *Proc. Int. URSI Symp. Electromagnetic Waves*, (Munich, Germany), Aug. 1980, Paper No. 341B.

[5] M. J. Shiau, H. Shigesawa, S. T. Peng, and A. A. Oliner, "Mode-conversion effects in Bragg reflection from periodic grooves in rectangular dielectric image guide," in *IEEE Int. Microwave Symp. Dig.*, (Los Angeles, CA), June 15–19, 1981, pp. 14–16

[6] S. T. Peng, A. A. Oliner, and F. Schwering, "Theory of dielectric grating antennas of finite width," presented at IEEE AP-S Int. Symp., Los Angeles, CA, June 1981.

[7] K. Solbach, "*E*-band leaky wave antenna using dielectric image line with etched radiating elements," in *1979 MTT-S Int. Microwave Symp Dig.*, Apr., 1979, pp 214–216.

[8] R. Mittra and R. Kastner, "A spectral domain approach for computing the radiation characteristics of a leaky-wave antenna for millimeter waves," *IEEE Trans. Antennas Propagat.*, vol. AP-28, pp. 652–654, July 1981

[9] T. Tamir, *Integrated Optics*. New York: Springer-Verlag, 1975.

[10] S. T. Peng, T. Tamir, and H. L. Bertoni, "Theory of periodic dielectric waveguides," *IEEE Trans. Microwave Theory Tech.*, vol. MTT-23, pp. 123, 1975.

[11] M. Neviere, R. Petit, and M. Cadilhac, "About the theory of optical grating coupler-waveguide systems," *Optical Comm.*, vol. 8, pp. 113–117, 1973.

[12] K. Honda, S. T. Peng, and T. Tamir, "Improved perturbation analysis of dielectric gratings," *Appl. Phys.*, vol. 5, pp. 325, 1975.

[13] S. T. Peng and T. Tamir, "TM-mode perturbation analysis of dielectric gratings," *Appl. Phys.*, vol. 7, pp. 35, 1975.

[14] T. Tamir and S. T. Peng, "Analysis and design of grating couplers," *Appl. Phys.*, vol. 14, pp. 235–254, 1977.

[15] R. F. Harrington, *Time-Harmonic Electromagnetic Fields*. New York: McGraw-Hill, 1961, pp. 106.

[16] S. T. Peng and T. Tamir, "Effects of grooves profile on the performance of dielectric grating couplers," in *Proc. Symp. Optical Acoustical Micro-Electronics*. Brooklyn, NY: Polytechnic Press, 1974.

[17] D. Marcuse, "Exact theory of TE-wave scattering from blazed dielectric gratings," *Bell Syst. Tech. J.*, vol. 55, pp. 1295–1317, 1976.

[18] K. C. Chang and T. Tamir, "Simplified approach to surface-wave scattering by blazed dielectric gratings," *Appl. Opt.*, vol. 19, pp. 282–288, 1980

[19] A. Gruss, K. T. Tam, and T. Tamir, "Blazed dielectric gratings with high beam-coupling efficiencies," *Appl. Phys. Lett.*, vol 36, pp. 523–525, 1980.

[20] H. G. Unger, *Planar Optical Waveguides and Fibers* Oxford, England: Oxford Univ. Press, 1978, ch. 3

[21] W. V. McLevige, T. Itoh, and R. Mittra, "New waveguide structures for millimeter-wave and optical integrated circuits," *IEEE Trans Microwave Theory Tech.*, vol. MTT-23, pp 788–794, Oct 1975.

[22] S. T. Peng and A. A. Oliner, "Guidance and leakage properties of a class of open dielectric waveguides: Part I—Mathematical formulations," *IEEE Trans Microwave Theory Tech.*, vol MTT-29, pp 843–855, Sept 1981.

[23] A. A. Oliner, S. T. Peng, T. I. Hsu, and A. Sanchez, "Guidance and leakage properties of a class of open dielectric waveguides: Part II —New physical effects," *IEEE Trans. Microwave Theory Tech*, vol. MTT-29, pp. 855–869, Sept. 1981.

[24] K. Ogusu and I. Tanaka, "Optical strip waveguide: An experiment," *Appl Opt*, vol 19, pp. 3322–3325, Oct. 1980.

Felix K. Schwering (M'60) was born on June 4, 1930, in Cologne, West Germany. He received the Dipl. Ing. degree in electrical engineering and the Ph.D. degree from the Technical University Aachen, Aachen, West Germany, in 1954 and 1957, respectively.

From 1956 to 1958 he was Assistant Professor at the Technical University, Aachen. In 1958 he joined the U.S. Army Research and Development Laboratory in Fort Monmouth, NJ, where he performed basic research in free space and guided propagation of electromagnetic waves. From 1961 to 1964 he worked as a Member of the Research Staff of the Telefunken Company, Ulm, West Germany, on radar propagation studies and missile electronics. In 1964 he returned to the U.S. Army Electronics Command, Fort Monmouth, NJ, and has since been active in the fields of electromagnetic-wave propagation, diffraction and scatter theory, theoretical optics, and antenna theory. Recently, he has been involved, in particular, in millimeter-wave antenna and propagation studies.

Dr. Schwering is a Visiting Professor at Rutgers University. He is a member of URSI Commission B and of Sigma Xi, and was a recipient of the 1961 Best Paper Award of the IRE Professional Group on Antennas and Propagation (jointly with G. Goubau).

Song-Tsuen Peng (M'74–SM'82) was born in Taiwan, China, on February 19, 1937. He received the B.S. degree in electrical engineering from the National Cheng-Kung University, in 1959, the M.S. degree in electronics from the National Chiao-Tung University, in 1961, both in Taiwan, and the Ph.D. degree in electrophysics from the Polytechnic Institute of Brooklyn, Brooklyn, NY, in 1968.

Since 1968 he has been with the Polytechnic Institute of New York and is currently a Research Associate Professor in the Department of Electric Engineering and Computer Science. He has participated in many research programs in cooperation with government and industrial laboratories in the U.S. and also in academic exchanges with universities abroad. He has carried out research in the areas of wave propagation, radiation, diffraction, and nonlinear electromagnetics, and has published numerous papers in electromagnetics optics and acoustics.

Dr. Peng is a member of Sigma Xi.

Theory of Optically Controlled Millimeter-Wave Phase Shifters

AILEEN M. VAUCHER, CHARLES D. STRIFFLER, MEMBER, IEEE, AND CHI H. LEE, MEMBER, IEEE

Abstract—**In this paper we analyze the millimeter-wave propagation characteristics of a dielectric waveguide containing a plasma-dominated region. Such a device presents a new method for controlling millimeter-wave propagation in semiconductor waveguides via either optical or electronic means resulting in ultrafast switching and gating. We have calculated the phase shift and attenuation resulting from the presence of the plasma. Higher order modes, both TE and TM, as well as millimeter-wave frequency variation, are studied in both Si and GaAs dielectric waveguides. We have also formulated a surface plasma model that is a good approximation to the more elaborate volume plasma model. Phase shifts are predicted to be as high as 1400°/cm for modes operating near cutoff. These modes suffer very little attenuation when the plasma region contains a sufficiently high carrier density.**

I. Introduction

WE ARE CURRENTLY witnessing a resurgence of interest in millimeter-wave technology. The frequency band extending from 30 to 1000 GHz is attractive in several respects. Devices operating above *K*-band frequencies offer greater carrier bandwidth, better spatial resolution, and a more compact technology than presently used *X*- and *K*-band systems. Millimeter- and submillimeter-wave systems also have some advantages over optical systems, such as better atmospheric propagation in selected bands and a technology more amenable to frequency multiplexing [1]–[3], while retaining good angular resolution of the latter. A basic problem is how to effectively preserve these benefits. Our approach to the solution of this problem promises to yield much larger modulation bandwidths than are realizable with optical systems, while preserving the economy of the millimeter-wave system over a given carrier frequency band.

One of the important parts of the microwave and/or millimeter-wave system is the waveguide. At microwave frequencies, metal waveguides are commonly used. At higher frequencies, either microstrip or dielectric waveguide structures become more attractive. Microstrip transmission lines are used up to 30 GHz. For frequencies greater than 30 GHz, the losses in microstrip structures are high, and fabrication techniques become more difficult due to the small strip width and the substrate thickness. Dielectric rectangular waveguides become an alternative to the expensive metal waveguides. The use of high-purity semiconductor materials as dielectric waveguides is particularly important since active devices such as oscillators, Gunn or IMPATT diodes, mixers/detectors, and modulators can be fabricated monolithically with the semiconducting waveguides.

Manuscript received May 3, 1982; revised August 6, 1982. This work was supported in part by the Harry Diamond Laboratory; the U.S. Army; the Minta Martin Aeronautical Research Fund, College of Engineering, University of Maryland; and the University of Maryland Computer Science Facility.

The authors are with the Electrical Engineering Department, University of Maryland, College Park, MD 20742.

0018-9480/83/0200-0209$01.00 ©1983 IEEE